January 2012

Atmospheric Mass Loss And Orbital Evolution Of Exoplanets

Nicole Thom

ATMOSPHERIC MASS LOSS AND ORBITAL EVOLUTION OF EXOPLANETS

By

Nicole Elizabeth Thom
Bachelor of Arts, Yale University, 2010

A Thesis
Submitted to the Graduate Faculty

of the

University of North Dakota

In partial fulfillment of the requirements

For the degree of

Master of Science

Grand Forks, North Dakota
August
2012

This thesis, submitted by Nicole Thom in partial fulfillment of the requirements for the Degree of Master of Science from the University of North Dakota, has been read by the Faculty Advisory Committee under whom the work has been done, and is hereby approved.

Dr. Michael Gaffey
Chairperson

Dr. Ronald Fevig

Dr. Brian Jackson

This thesis is being submitted by the appointed advisory committee as having met all of the requirements of the Graduate School at the University of North Dakota and is hereby approved.

Wayne Swisher
Dean of the Graduate School

Title   Atmospheric Mass Loss and Orbital Evolution of
                 Exoplanets

Department   Space Studies

Degree   Master of Science

In presenting this thesis in partial fulfillment of the requirements for a graduate
degree from the University of North Dakota, I agree that the library of this
University shall make it freely available for inspection. I further agree that
permission for extensive copying for scholarly purposes may be granted by the
professor who supervised my thesis work or, in his absence, by the Chairperson
of the department or the dean of the Graduate School. It is understood that any
copying or publication or other use of this thesis or part thereof for financial gain
shall not be allowed without my written permission. It is also understood that
due recognition shall be given to me and to the University of North Dakota in
any scholarly use which may be made of any material in my thesis.

                                    Nicole Thom
                                    7/26/2012

TABLE OF CONTENTS

LIST OF FIGURES

ACKNOWLEDGEMENTS

ABSTRACT

The distributions of the semi-major axes and masses of close-in planets (planets within 0.1 AU of their host stars) provide clues to their origin. Over billions of years, the mass and orbital distance are constantly evolving. Tidal forces and atmospheric mass loss, driven by stellar ultraviolet flux, can influence the observed planetary distribution. Coupling these effects can lead to a greater understanding of how the observed distribution was shaped and may help to explain the gaps in the distribution of mass and semi-major axes for these close-in planets.

To study the effects of mass loss and tides, we applied a numerical model to many hypothetical populations of close-in planets and compared these hypothetical populations to the observed population. The evolutionary paths determined by the model depend on two as of yet poorly-constrained factors: the tidal dissipation factor (Q_*) and the heating efficiency (ε). By statistically comparing the observed distribution of close-in exoplanets with the hypothetical population, modeled under different ε and Q'_* conditions, these values are tested. Under all conditions the two populations were statistically dissimilar, indicating that the population was either not initially evenly distributed, or that there is another important factor in planetary evolution.

CHAPTER 1

INTRODUCTION

History

The book on planet formation has been completely rewritten with the discoveries of hundreds of exoplanet systems. For example, close-in exoplanets, planets within 0.1 AU of their host stars, seem to be common among extra-solar systems but do not exist in our own solar system. These planets probably formed much farther from their host stars, and interactions with their maternal gas disks or with their sibling planets drove them to their current close-in orbits (Lin et. al., 1996, Rasio et al., 1996, Dobbs-Dixon et al., 2004).

The distribution of their semi-major axes and masses can provide clues as to which migration scenario occurred, but only to the extent that other evolutionary effects can be accounted for. In particular, tidal forces (caused by tides being raised on the star by the planet) and atmospheric mass loss caused by stellar ultraviolet flux can shape these distributions.

Atmospheric mass loss is simply the reduction in a planet's atmosphere. While there is not a consensus that energy-limited atmospheric escape, meaning atmospheric escape that is driven by the amount of energy put into the system by XUV flux, plays a dominant role in the mass evolution of exoplanets (Yelle, 2004; Hubbard et al., 2007), there have been many models suggesting its importance (Erkaev et al., 2007, Lammer et al., 2003, Sanz-Forcada et al., 2011

1

among others). The mass loss process is likely driven by the X-ray and Extreme-Ultraviolet (XUV) irradiation (0.1 to 100 nm in wavelength) from the exoplanet's host star (Hubbard et al., 2007; Lammer et al. 2003).

While the exact composition of an exoplanet may not be known, the mass and radius measurements of many exoplanets suggest an atmosphere composed in large part of hydrogen and helium (Rogers and Seager, 2010). Mass loss of these elements has been shown to play a significant role in the evolution of some planetary systems, through direct observation in an exoplanet system (Vidal-Madjar et al., 2003), and even in models of our own early solar system (Kulikov et al., 2006).

The amount of XUV energy that is used for mass loss is dependent, in part, on the depth of radiation absorption (Cecchi-Pestellini et al., 2009). The effects of the XUV radiation are only important in the upper atmosphere. However, not all of the XUV energy arriving at the upper atmosphere is used to drive mass loss. The value of the heating efficiency, or the fraction of energy being used to excite the upper atmosphere, affects the estimations of mass loss. Estimations have ranged from as high as 0.5-0.6 (Yelle, 2004), meaning 50-60% of the incoming radiation is driving mass loss, to a lower value range of 0.1-0.25 (Lammer et al., 2009).

Even low estimates of hydrodynamic mass loss suggest that it is a significant factor for close-in exoplanets. Mass loss rates have been estimated to be from 10^5 g/s to 10^{12} g/s (Lecavelier des Etangs). Lammer et al. (2009) found that significant mass loss (more than 1% of the planet's initial mass) occurs in planets less than 0.02 AU from their host star. At extremely close distances, less

than 0.015 AU, low density, sub-Jupiter sized planets may lose their entire atmospheres.

In addition to a dependency on the proximity of the host star, the size of the planet also dictates the rate of mass loss. The mass and radius of a planet are factors in the surface gravity of the planet. The surface gravity plays a major role in determining the mass loss rate – planets with a higher surface gravity have a slower rate of mass loss. Another important factor for mass loss is the system's age. When a star is young, the radiation given off in the XUV wavelengths stars out high, and drops off over time. As the star ages, the rotation rate slows down substantially (Simon et al., 1985). The XUV emission is tightly correlated to the rotation rate of the star. This correlation only works up to a certain point, when the luminosity becomes saturated relative to the rotation rate (Pizzolato et al., 2003).

While close-in exoplanets are more susceptible to XUV-driven mass loss, it has been suggested that planets up to 1 AU could experience hydrodynamic mass loss during the early history of the star (Lammer et al., 2003). Even though some close-in exoplanets are believed to have an intrinsic magnetic field, the young stars may have a strong enough XUV flux to overcome it and cause significant mass loss (Greißmeier et al., 2004). The smaller than expected number of observed planetary masses near their star indicates the XUV flux played a dominant role in planetary evolution, as these planets would have been evaporated away. This would be an especially large effect in the early stages of the planet formation, as that is the time when they would have experienced the strongest XUV flux (Sanz-Forcada et al., 2010; Sanz-Forcada et al., 2011).

Another stellar property, mass, is an important factor for planetary mass loss estimations. The evolution of G-type stars has been studied in detail with the Sun in Time program. This program looks at a series of solar analog stars of ages ranging from 0.1-7 Gyr to track the evolution of their X-ray and ultraviolet radiation (Ribas et al., 2005). The stars range from type G0-G5 V. The stars chosen have well-known temperatures, luminosities, metallicities, and ages. While the initial Sun in Time program looked at over 15 solar proxies, Ribas et al. focused on 7 stars (including the sun) to study the XUV evolution.

From the study of this sample of stars, Ribas et al. were able to determine a relationship between the flux and stellar age. They determined that the emissions from the youngest sample stars at all XUV wavelengths were at least an order of magnitude larger than the sun's current flux. The youngest star observed had emissions 100 times larger than the sun's present value. This demonstrates that the XUV output of sun-like stars is extremely high, but drops off quickly within the first Gyr.

The results from this project have been widely used to model XUV evolution of G-type stars. However, this is not the only method for determining the XUV radiation levels. Synthetic spectra can be generated to simulate the emissions of stars of different masses (Sanz-Forcada et al., 2011). Additionally, Penz et al., (2008) used the ages of star clusters to derive a scaling law for the population of G-stars (taking into account only X-ray and not ultraviolet emissions). This model was then applied to an energy-limited mass loss model to determine the atmospheric mass loss of close-in exoplanets. They found a large range of X-ray luminosities, leading to a wide range of evaporation histories.

High-energy stars were found to be able to evaporate the atmospheres of planets up to 0.5 AU; however, moderate X-ray luminosities had a much smaller effect.

The work done in the Sun in Time program is now being used as a model to understand the XUV evolution of other types of stars (DeWarf et al., 2010). This will lead to an understanding of mass loss for a broader range of exoplanet systems.

While mass loss has been theorized for many exoplanets, the best studied exoplanet has been HD 209458 b. Lammer et al. (2003) used their equations to estimate that this planet is losing mass at a rate of $\approx 10^{12}$ g/s. They further noted that Jeans escape would account for a mass loss of less than 1 g/s for a similar temperature.

This estimate fits in with the value observed by Vidal-Madjar et al. (2003). This group made observations of HD 209458's Lyman-alpha lines when the planet was transiting across it. They noted that there was an absorption of hydrogen during the transits. By comparing the observed absorption with models, they concluded that the planet likely has an extended Roche lobe. They also showed that the atoms being observed in the spectrum were moving at a high velocity when compared to the planet. Considering all of the data, they concluded that HD 209458 b is losing mass at a minimum rate of 10^{10} g/s, and acknowledged that the rate could be several orders of magnitude larger than that because a sufficiently large density of gas is escaping, causing the Lyman-alpha feature of the spectrum to become saturated.

In addition to mass loss, close-in exoplanets are experiencing orbital migration. The orbital distance for these exoplanets is strongly affected by tidal

interactions with the host star. The tides of planets with an orbital period of less than the star's rotation period will transfer angular momentum from their orbit to the stellar spin, resulting in migration toward the star (Rasio et al., 1996). The angular momentum is transferred from the orbit of the planet to the stellar rotation. However, the system is losing total angular momentum due to the stellar winds, further reducing the semi-major axis. This migration toward the star will continue until the planet approaches too close to the star and is pulled apart through the tidal forces.

Exoplanet evaporation is believed to be one culprit behind the "lost population" of exoplanets (Davis and Wheatley, 2009). This lost population can be seen when plotting the mass against the semi-major axis of the observed exoplanets. There is an absence of planets of less than 0.013 AU with masses less than a Jupiter mass. These gaps cannot be explained by observational biases, as the missing planets would be observable if they were there.
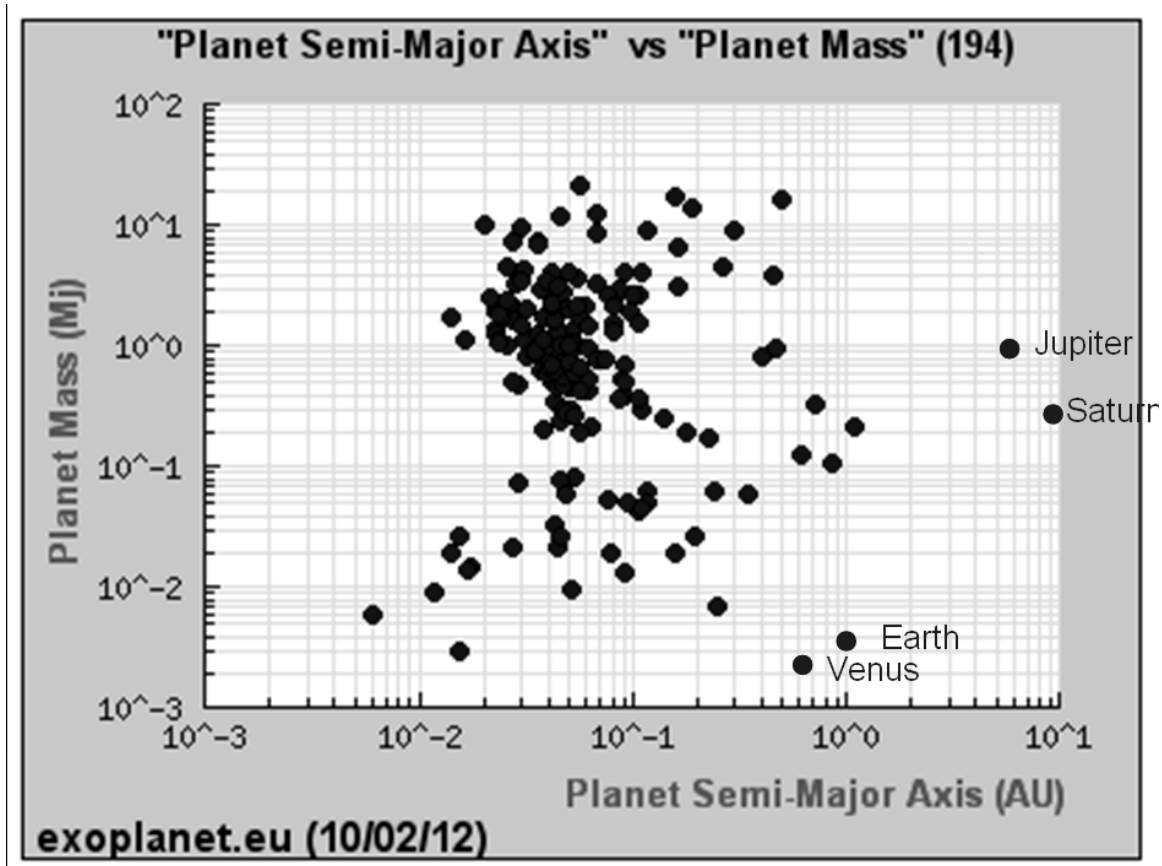
Figure 1: Distribution of Transiting Planets. Plot of the semi-major axis and mass of the observed transiting planets. The planets in the solar system are also plotting as a reference. There is a noticeable gap in planets at close-in distances (less than 0.03 AU) with masses from 0.1-1 Jupiter masses.

These planets may have already been removed from the population, and therefore are not seen today. Planets whose atmospheres approach the planet's Roche lobe were likely already destroyed as a result of both mass loss and orbital evolution.

Another outcome of mass loss is the formation of smaller, denser close-in planets. If hot Jupiters lose their mass at a high rate, they will eventually become smaller objects, such as Neptune-like planets or even small rocky bodies (Vidal-Madjar et al., 2003).

Recent studies have begun to look at how the XUV driven mass loss and tidal evolution are linked. The evaporation of planets has been shown to play a role in tidal evolution by affecting the size of the tides (Guo, 2010). In turn, tidal evolution would have an effect on mass loss by increasing the XUV flux as the orbit moves inward. During the early stages of a planet's life, mass loss would play a dominant role because of the initial high XUV radiation rate from the star. As the planet ages, the XUV-driven mass loss would become less significant and orbital evolution would become more prominent. As the planet moves closer, it raises larger tides on the star, increasing the tidal evolution effect. Therefore, understanding the relationship of these two factors is essential to understanding the evolution of the observed exoplanet distribution.

CHAPTER II

METHODS

2.1 Mass Loss

Planetary atmospheres are not constant features; they are being lost over time. Observations of other planets show that they are losing mass at varying rates. Atmospheric mass loss is defined as the rate at which the atmosphere of a given exoplanet is being removed. For close-in exoplanets, mass loss is driven primarily by stellar X-ray and ultra-violet (XUV) flux (wavelengths from 0.1 to 100 nm) from the host star. This XUV radiation

ionizes and heats the hydrogen gas in the atmosphere, giving it the energy to escape the gravitational pull of the planet.
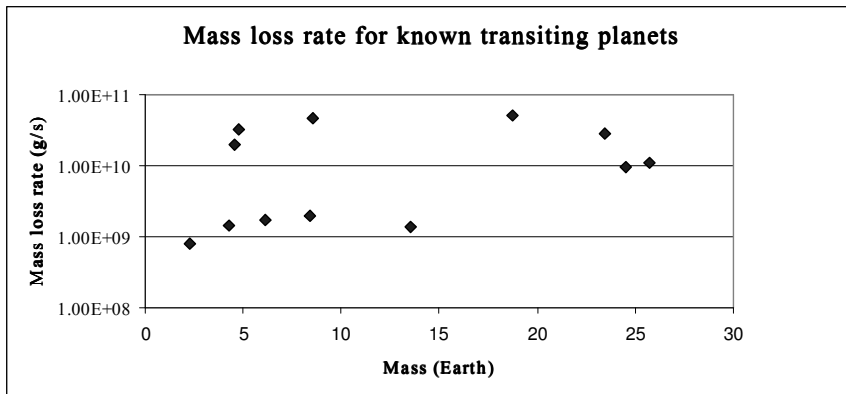

Figure 2: Mass Loss Rates. Example of the rate of atmospheric mass loss for observed transiting planets. Note that the planets undergoing the strongest mass loss are losing atmosphere at a rate on the order of 1×10^{10} g/sec.

The total atmospheric mass loss can be represented by dividing the XUV flux received at the surface of the planet by the amount of binding energy that the planet has. If energy is entering the system at a great enough rate, the particles in the atmosphere are not stable and are able to be released from the gravitational pull of the planet. An approximation of the amount of mass loss can be determined by relating the rate of energy input to the change in the gravitational energy needed to for a particle to escape (Jackson et al., 2010). Erkaev et al. (2007) estimated this using the equation

$$\frac{dM_p}{dt} = -\frac{\pi R_p^3 \varepsilon F_{XUV}}{GM_p K_{tide}}$$ (1)

where R_p is the radius of the planet, ε the fraction of incoming energy that drives mass loss, F_{xuv} the XUV flux, G the gravitational constant, M_p the planet's mass, and K_{tide} the reduction in escape energy due to the star's tidal gravity. Both ε and K_{tide} are values that lie between 0 and 1. A more detailed description of these parameters follows.

As discussed previously, the XUV flux is not a constant value. As stars age, they lose angular momentum because of magnetic braking (Skumanich et al., 1772; Ivanova and Taam, 2003). The drop in angular momentum leads to a subsequent increase in the rotation period. The stellar dynamo decreases as a consequence of the increased rotation period, leading to a reduction in the emission at the XUV wavelengths important for mass loss (Zahnle and Walker, 1982). Therefore, as the star ages, there is an overall decrease in the star's XUV emission. The rate at which this occurs is dependent on the stellar type. A

detailed study of several G-type stars was conducted, leading to the relationship

given by (Ribas et al., 2005)

$$F_{XUV} = \lambda t_{Gyr}^{-\beta} / a^2 \qquad (2)$$

Where λ = 29.7 erg/s/cm^2, t is the age in Gyr, β = 1.23, and a is the semi-major axis. This relationship was found using stars between the ages of 0.1 and 6.7 Gyr.

ε is a parameter that represents the fraction of incoming energy that drives mass loss. If all of the incoming energy is used to drive mass loss, ε will have a value of 1. However, if some of the incoming energy is driving other processes, such as driving chemistry processes in the atmosphere, the value will be lower (Yelle, 2004).   Several estimates of ε have been made. For example, Lammer et al. (2009) suggest that, for a hydrogen-rich gas giant, the column-averaged heating efficiency should be less than 0.6, and more likely around 0.25. For this study, a range of ε values spanning the range of estimated values (ε= 0.001 0.1, 0.25, 0.5, and 1) was used in order to further constrain the likely values.

The K$_{tide}$ parameter is a measure of the reduction in the escape energy required due to the star's gravity. For atmospheric particles to escape, they need only to reach a position where the particles are no longer bound to the planet. This boundary is known as the Roche lobe. This factor can be represented by the equation

$$K_{tide} = 1 - \frac{3}{2\xi} + \frac{1}{2\xi^3} \qquad (3)$$

Where

$$\xi = \frac{\left(\left(\frac{M_p}{3M_*} \right)^{\frac{1}{3}} \alpha \right)}{R_p} \tag{4}$$

where M_p is the planetary mass, M_* is the stellar mass, R_p is the planetary radius, and a is the semi-major axis (Erkaev et al., 2007).

2.2 Tidal Evolution

Just as the moon raises a tide on Earth, close-in planets raise significant tides on their host stars. The majority of stars that host a planet have a spin period that is greater than the surrounding planet's orbital period. The gravitational interaction between the planet and the tidal bulge that is raised on the star results in a tidal torque which transfers energy and angular momentum between the star and the planet (Murray and Dermott, 1999). The result is that the semi-major axis slowly decreases.

The model used for the orbital evolution is

$$\frac{da}{dt} = -\frac{9}{2}(G/M_*)^{1/2} \frac{R_* M_p}{Q'_*} a^{-11/2} \tag{5}$$

where M_* is the stellar mass, R_* is the stellar radius, M_p is the planetary mass, Q'_* is the modified tidal dissipation factor, and a is the semi-major axis (Murray and Dermott, 1999).

The magnitude of the tidal torque bulge depends on the tidal dissipation factor (Q). As Q often appears in theory in combination with other factors, it is often identified as Q', which incorporates the Love number (which measures the interior density profile of the star) (Ogilvie and Lin, 2007). The larger the Q'

value, the smaller the effect of tidal evolution of the planet's orbit. While several attempts have been made to constrain the value of Q_*, the tidal dissipation factor of the star, it is as of yet uncertain (Penev et al., 2011). Recently, Penev et al. (2012) have suggested that $Q_* > 10^7$. Tidal evolution can have an impact on mass loss in that the closer the planet is to the star, the more XUV flux the planet receives, which increases mass loss from the planet.

2.3 Code Description

For this project, I used a modified version of the planetary evolution code utilized by Jackson et al. (2010). This program numerically integrates the tidal and mass evolution equations.

The code is broken up into two segments. The first segment takes the observed properties of the exoplanet as they are currently observed and integrates "back in time" to simulate the history of the planet. The second segment is similar, but instead of giving the history of the planet, it runs forward in time from the current properties and returns what will happen to the planet in the future with the given input parameters.

For each segment of the code, the beginning conditions for the planetary system are required. For stellar parameters, the stellar mass, radius, and Q_* value are needed.

Planetary properties include the mass, core mass, and semi-major axis. The planetary radius is determined by calling another subroutine which takes the planetary mass, core size, semi-major axis, and age. This routine then interpolates between the different values in a table of values in order to find the closest radius

estimate (Miller et al., 2009). A more detailed explanation of these tables can be found in the next section.

There are also several additional requirements. The first of these is the minimum or maximum age, depending on whether the program is running backward or forward in time, respectively. For this code, the minimum age was set to 1×10^8 yr. This age was selected as it is the cutoff used for the Sun in Time program. Before that age, the star's XUV flux is significantly higher and more variable (Ribas et al., 2005). By setting the minimum time to 100 Myr, the model provides a conservative estimate of the total mass lost by the modeled planet. The maximum age was set to 10 Gyr, the typical lifetime of a G-type star.

The minimum semi-major axis and planetary mass parameters are also essential components for the code. If the semi-major axis is within 0.5% of the stellar radius, the code will stop and return the values.

Once all of the input parameters are entered, the code determines the Roche radius of the planet. As long as the Roche radius is greater than the planetary radius and the age is not yet to 10 Gyr, then the code will calculate the XUV flux reaching the planet, the K_{tide} value, the amount of mass loss, and the change in semi-major axis. Each of these elements is determined by calling a separate function that returns the values using the equations listed above. The code then updates the values for the planet's age, mass, semi-major axis, radius, and Roche radius.

As long as the Roche radius is larger than the planetary radius and age is less than 10 Gyr, the program continues to call the subroutine. From this, the

age, mass, radius, and semi-major axis is determined from the input planet's current conditions back to 1×10^8 yr (or forward to 10Gyr).

2.4 Miller Tables

The tables used to determine R_p as a function of planetary age, M_p, and core mass came from Miller et al., (2009). The composition of the core was assumed to be 50% rocky material and 50% ice, while the atmospheric envelope is made of hydrogen and helium. Note that the choice of core composition has no effect on the planetary radius while the planet is a gas giant. Only after the mass is reduced to the core mass do these assumptions have an effect. The table was computed by holding the mass, core mass, and semi-major axis constant and then computing the radius at which the atmospheric pressure is 1 bar. The change in the radius is caused by cooling of the planet, which leads to contraction.

The tables are limited in the ranges for different parameters, namely the mass, semi-major axis, and age of the planetary system. The table extends from $M_p = 0.035$ to $M_p = 10$ M_{jup}; the semi-major axis extends from $a = 0.01$ AU to 0.15 AU; and the age extends from 0.1 Gyr and 4.59 Gyr.

The range of ages provided by the table is significantly smaller than the range of ages that are modeled. Even when the age of the system is estimated to be less than 4.59 Gyr, the future evolution of the planet is cut off at that point, which limits the information we can learn about the path the planetary system will follow if the age is only slightly below the cutoff. The planetary radius contracts asymptotically with increasing age. Beyond 4.59 Gyr, this contraction is

15

negligible. Therefore, for values between 4.59 Gyr and the set maximum age of 10 Gyr, the code assumes an age value of the planet of 4.59 Gyr.

Because the majority of the cooling of the planet happens in the first Gyr after formation, the radius only marginally declines after that point. However, the XUV flux from the star would decrease with age. This would have an impact on the system, but again, the older the star is, the less the XUV flux changes.

2.5 Test cases

The life span of a population of planets can me modeled , and the evolution simulated, by coupling the mass loss and orbital evolution equations. The evolutionary track of several observed exoplanets was modeled as illustrative examples.

The first planet chosen was HAT-P-25b. The values of M_*=1.01 solar masses, R_*=0.959 solar radii, M_p=0.567 M_{jup}, a=0.0466 AU, and the age, t=3.2 Gyr were taken from Quinn et al. (2012).

Our model suggests that HAT-P-25 b is undergoing mass loss, but at a very slow pace. There are two reasons: HAT-P-25 b is relatively far from the host star, resulting in a lower XUV flux at the planetary surface. Additionally, the planet is fairly massive, and therefore has a stronger gravitational hold on its atmosphere.

The second observed planet that fit the restrictions was WASP-19 b. This exoplanet is much closer to its host star (0.01655 AU compared to 0.0466 AU). Other system characteristics used were M_*=0.97 solar masses, R_*=0.99 solar radii, and M_p=1.168 M_{jup} (Hellier et al., 2011). The age of the system is known to be

greater than 1 Gyr, so this is the value used in the calculation. The results of this calculation are shown below, again using $Q_*=10^7$ and $\varepsilon=1$.

Note that for this planet, the calculations were not carried all the way out to 10 Gyr. Instead, the calculation ends at around 1.055 Gyr. This indicates that, in the near future, WASP-19b may be disrupted, coming close enough to its host star that the planet fills its Roche lobe. This is a reasonable outcome because of the small semi-major axis, which leads both to large tidal effects and large XUV flux input. Additionally, the system is relatively young in age, so the XUV flux output from the star is still high.

It is important to keep in mind the use of $\varepsilon=1$ for both of these planets. This means that the code is assuming that all of the incoming flux is being used to drive mass loss. Thus, the mass loss rate is probably significantly overestimated. Nonetheless, there is likely a significant amount of mass loss currently occurring from WASP-19 b.
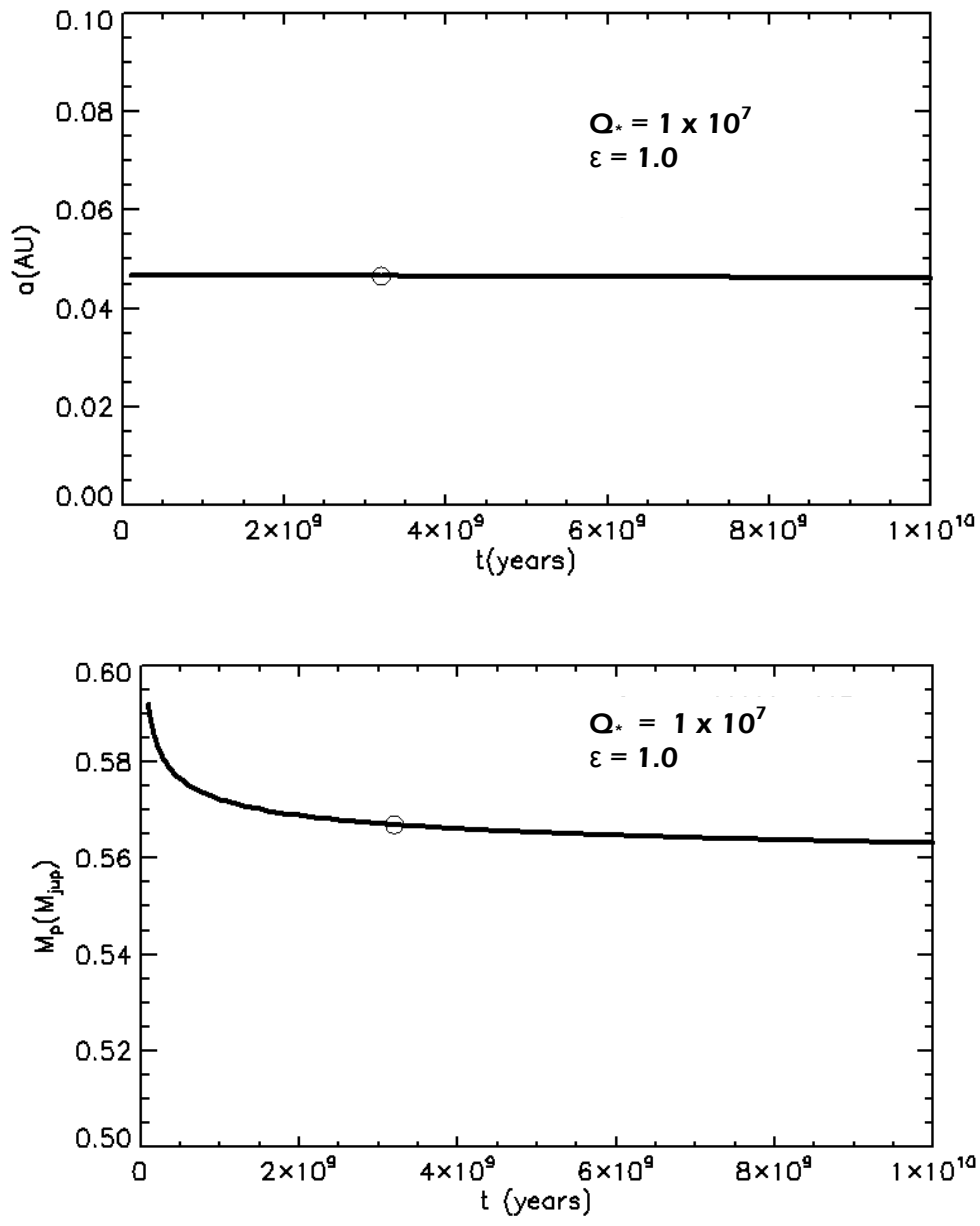
Figure 3: Mass and Semi-major Axis Evolution of HAT-P-25 b. Top figure- semi-major axis evolution of HAT-P-25 b. There is a minimal amount of orbital migration over the lifetime of this planet. Bottom figure – Mass evolution of HAT-P-25 b. The mass evolution begins quickly in the first 2 billion years, but then levels off as the system ages. The circle represents the current parameters for the system.
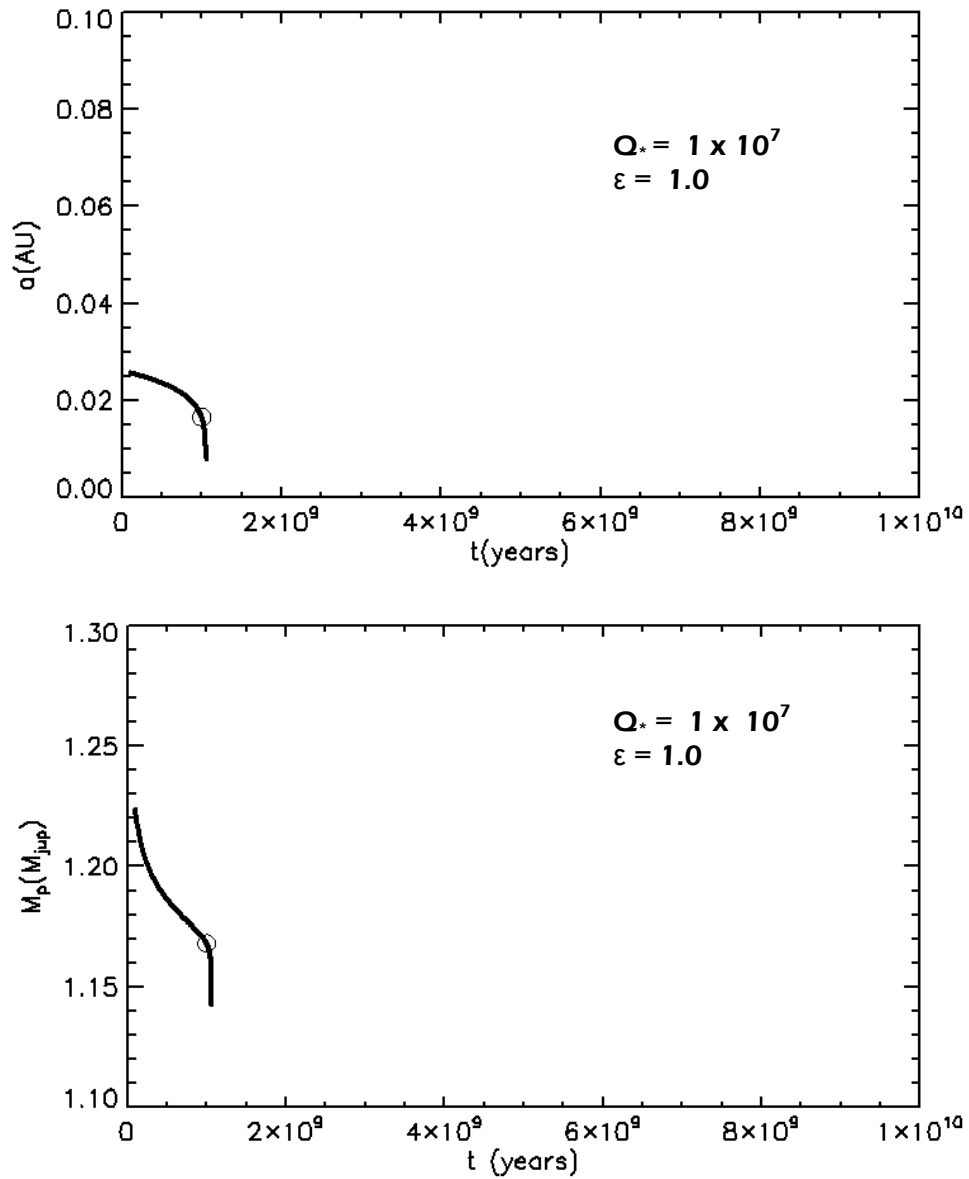
Figure 4: Mass and Semi-major Axis Evolution of WASP-19 b. Top figure- semi-major axis evolution of WASP-19 b. There is rapid evolution due to the planets close distance and large mass. Bottom figure – Mass evolution of WASP-19 b. The mass evolution is also significant, as nearly 5% of the initial mass has already been lost. Mass loss continues rapidly in the near future as the decreases semi-major axis leads to an increased level of XUV flux at the surface. The circle represents the current parameters for the system.

2.6 Limiting Cases

It is also important to constrain how much mass loss and evolution we would expect to see in a given population of exoplanets. We consider 4 limiting cases. The mass range determined was $0.052 < M_p < 9.1$ M_{jup}, representative of the observed exoplanets with semi-major axes greater than 0.1 AU. At these distances, the planets experience negligible mass loss and so, presumably, their mass distribution represents the original distribution for close-in planets.

The maximum semi-major axis considered for this work was 0.1 AU. The minimum semi-major axis test case uses a value of 0.02 AU.

The results for the planetary mass, radius, and semi-major axis history can be seen in the figures below. These charts were produced using an epsilon value of 1. Similar calculations were carried out with different epsilon values, but all produced a similar evolution. However, the minimum mass - maximum semi-major axis case was the exception. In this case, there was a 0.01 M_{jup} difference in mass loss over the 4 Gyr the simulation covered.
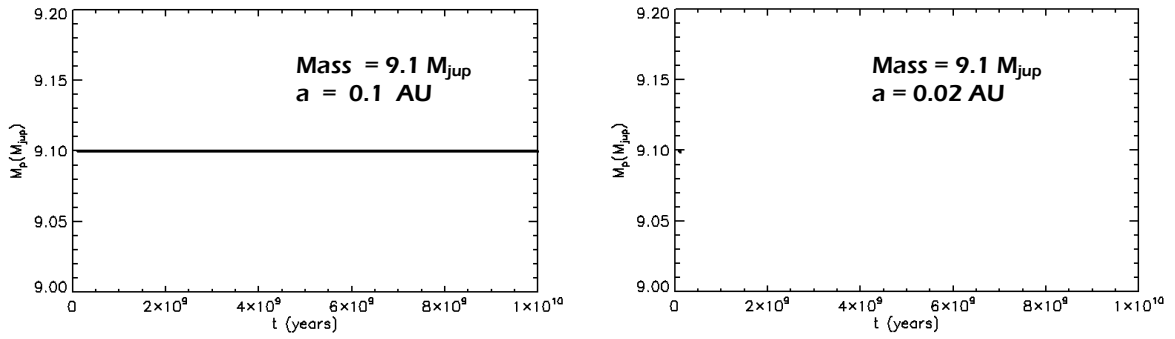
Figure 5: Mass Loss Evolution for a 9.1 M_{jup} Planet. Mass loss for an exoplanet with the maximum mass considered. The left shows the mass loss is negligible for a starting distance of 0.1 AU from the star. On the right, the small dot represents near the starting mass indicated that the planet is destroyed quickly after formation.
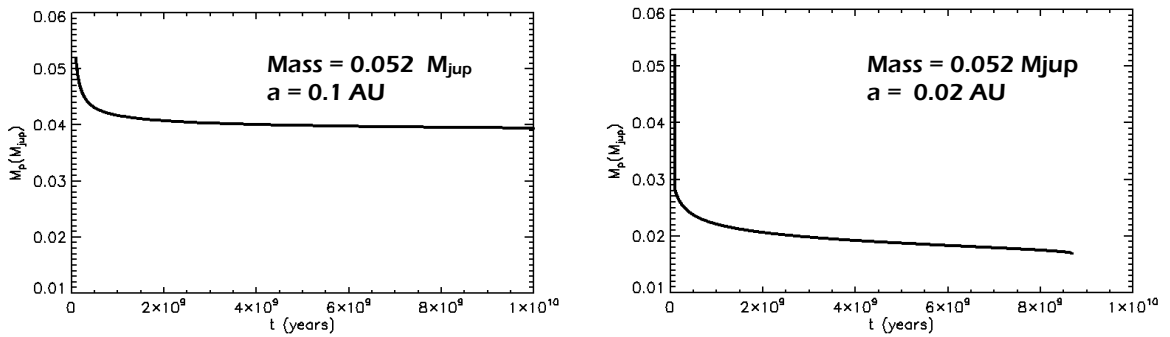

Figure 6: Mass Loss Evolution for a 0.052 M_{jup} Planet. Mass loss for an exoplanet with the minimum mass considered. The left shows the mass loss is about 20% for the planet if it began at a distance of 0.1 AU from the star. However, it loses around 60% of its mass when started from a distance of 0.02 AU. For both situations, the mass loss starts of quickly and drops to a steady rate after around 1 Gyr.
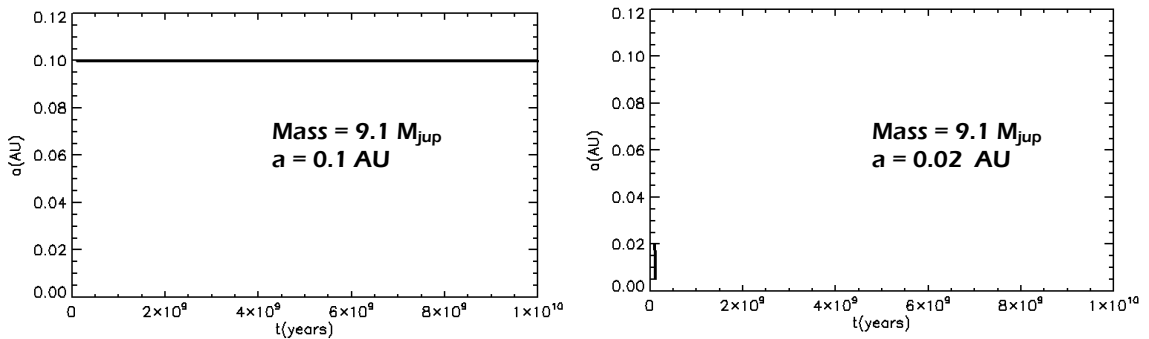

Figure 7: Semi-major Axis Evolution for a 9.1 M_{jup} Planet. Evolution of an exoplanet with the maximum mass considered here with a comparatively large (left) and small (right) semi-major axis. When the semi-major axis is large, there is little change over 10 Gyr. However, with a beginning semi-major axis of 0.02 AU, the planet quickly migrates inward and is destroyed.
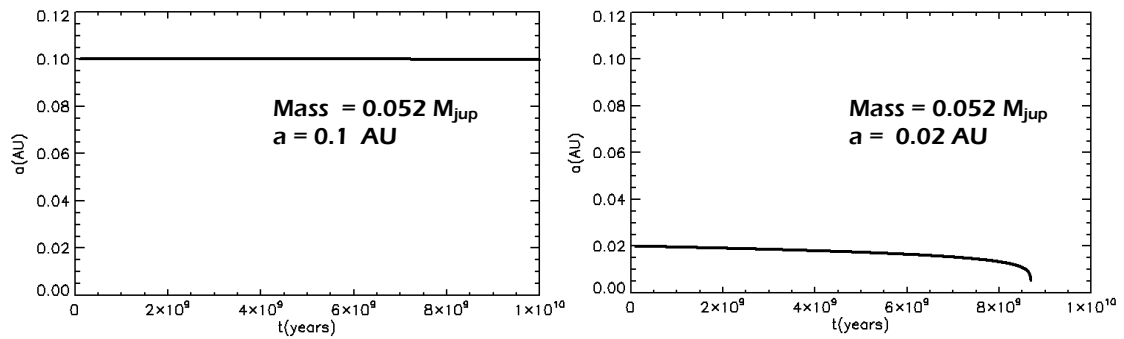
21

Figure 8: Semi-major Axis Evolution for a 0.052 M_{jup} Planet. *Evolution of a small-mass exoplanet with a semi-major axis of 0.1 AU (right) and 0.02 AU (left). When the semi-major axis is large, there is little change over 10 Gyr. However, at a small semi-major axis, the planet spirals inward slowly, and is eventually destroyed at around 8.6 Gyr.*

As can be seen from figures 5-8, the mass loss is most significant early in the planet's life, as the stellar XUV flux is the largest at a young age. As the XUV flux decreases, the mass loss also begins to taper off. The exception is the case of the 9.1 M_{jup}, 0.01 AU planet. The mass loss for this system increases rapidly until the planet falls into the star due to the rapid reduction in the semi-major axis. As the planet moves inward, the XUV flux received at the planet's surface increases more rapidly than the aging star's XUV flux decreases. Additionally, the K_{tide} value decreases as the planet moves inward, exacerbating the planet's mass loss.

The semi-major axis evolution is closely tied to the distance from the host star. Figures 7 and 8 show that the two most distant test cases, with initial semi-major axes of 0.1 AU, show very small amounts of orbital evolution for the selected value of Q'_*. Note that choosing a smaller Q'_* value could lead to stronger orbital evolution. However, the minimum semi-major axis test cases show more rapid decay of their orbits. The closer the planet is to the star, the larger the tides formed on the star. In addition, the smaller orbital periods mean

the rate of tidal dissipation (which scales with the orbital frequency) increases, likewise increasing the decay rate. Larger tides then lead to more rapid orbital evolution. For the 9.1 M_{jup}, 0.01 AU planet, the tidal evolution causes the planet to fill its Roche lobe and be disrupted within a few tens of millions of years. The large mass of the planet creates significant tides on the star, leading to more rapid evolution than the case with the same initial a but smaller initial M_p.

2.7 Hypothetical Population

With the extreme cases established, the next step is to create a population of exoplanets that fall within those limits in order to see how they evolve according to the model. The Q′$_*$ and ε values used for modeling the hypothetical population's evolution can be varied. Therefore the evolutionary outcomes will differ depending on which values are chosen. The different outcomes for the hypothetical population can then be compared to the observed population's distribution. Determining which evolutionary track's distribution for the hypothetical population most closely resembles the observed distribution will lead to constraints on the Q′$_*$ and ε values.

Since the mass loss code used in this paper requires that the host star be of G type, the stellar mass was randomly generated using numbers that fit in with the G-type star range, between 0.906 and 1.04 M_* (Habets et al., 1981).

These masses were then used to calculate the radii of the stars using the equation

$$\log(R_*/R_{sun}) = 0.917 * \log(M_*/M_{sun}) - 0.20 \qquad (6)$$

valid for $-1.0 < \log(M/M_{sun}) < 0.12$ (Lang, 1991 from Harris et al., 1963). Figure 5 compares this equation's results to observed planet-hosting stars. Note that the formula consistently underpredicts the radius. This means that the model will in turn underpredict the rate of orbital decay.

Because the radii generated in this manner became increasing discrepant the larger the mass became, a better relationship was desired. Therefore, a 2nd degree polynomial fit was done. This resulted in the relationship

$$R_* = 0.6355 * M_*^2 + 0.2505 * M_* + 0.1651 \tag{7}$$

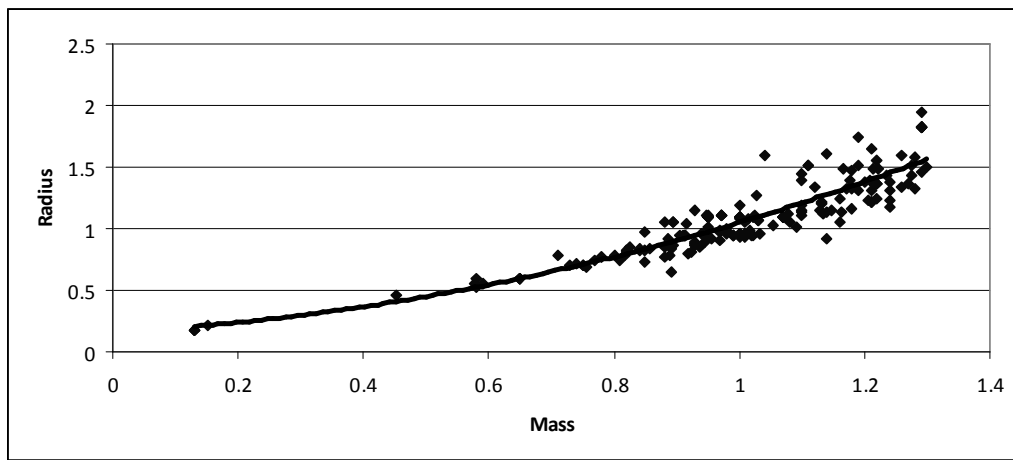The results of this calculation are shown below.

Figure 9: Comparison of Observed and Derived Stellar Radii. *Graph of the distribution of the mass and radii of the observed population (diamonds) and the 2nd degree polynomial fit to the data (black line). Mass is measured in solar masses, and radius is in solar radii.*

To determine the planetary mass range, all of the planets in the exoplanet encyclopedia (http://exoplanet.eu/) discovered by the transit method with a semi-major axis larger than 0.1 AU were compiled on April 6, 2012. As these planets are farther away from their host stars, they likely have not undergone a significant amount of mass loss, and therefore more closely resemble the original mass distribution.

These values ranged from a mass of 0.052 for Kepler-18d to Kepler-30c at 9.1 M_{jup}. On the low mass end, Kepler-11c, d, e, and f as well as Kepler-20f were removed because they are smaller than the models account for, and their low mass indicates a rocky composition, for which mass loss is not as likely. Also, both KOI-423 b at 18 M_{jup} and Kepler-30 d at 17 M_{jup} were eliminated because their size puts them in a region where their mass cannot be sufficiently distinguished from a brown dwarf star (Bouchy et al., 2011; Fabrycky et al., 2012). Kepler 27 b and c (9.11 and 13.8 M_{jup} respectively) were also eliminated, as they are as of April 6 unconfirmed.

The semi-major axis for each planet in the hypothetical population is a randomly generated number with a uniform probability to lie anywhere between 0 and 0.1 AU. After the stellar mass, planetary mass, and semi-major axis were generated, the Roche limit of the system was determined. If the planet moves inside of the Roche limit, it will be broken apart by the tidal forces of the star. Planets beginning within 1% of this limit were eliminated from further calculations.

The final age of each planet was also generated, creating a random population with a final age distribution similar to what we actually observe. This was done by choosing random planetary ages with probabilities given by the distribution of ages from Takeda et al., (2007). In this paper, a uniform distribution of star ages was assumed before applying a Bayesian fitting routine.
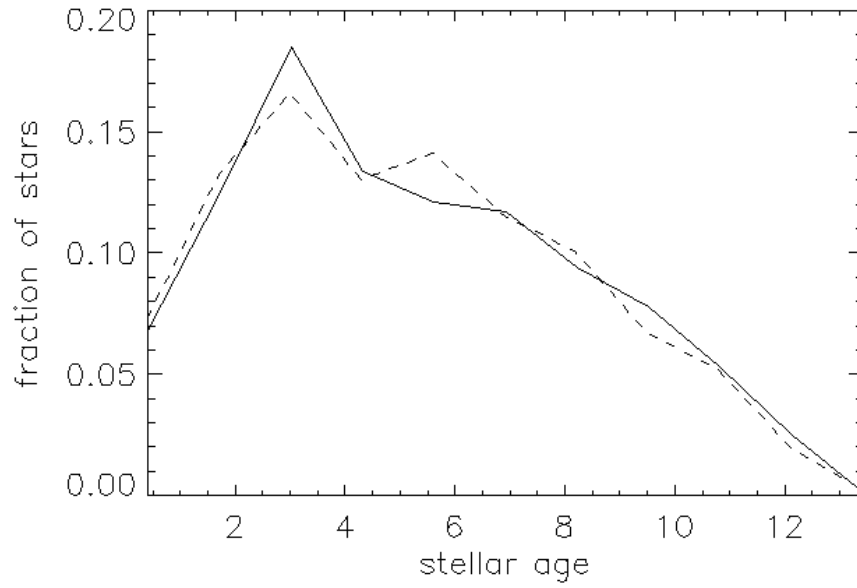
Figure 10: System Age Distribution. Histogram of the stellar population for the observed population used in Takeda et al. (2007) (dashed line) and the randomly generated population (solid line).

Other values of the hypothetical population were kept constant over the entire population. The core mass of all of the planets was assumed to be 9 Earth masses. The initial age of each of the planets was 0.1 Gyr, and the evolution of the population was tracked from that time to the randomly generated final age described above.

CHAPTER III

RESULTS

Several runs were made with the hypothetical population to constrain the ε and Q'$_*$ factors. The ε values used were 0.001, 0.1, 0.25, 0.5, and 1. The tidal dissipation was chosen as 10^5, 10^6, 10^7, and 10^8. The entire hypothetical population was evolved for each possible set of these values.

This population was evolved under these conditions until each planet either made it to the age attributed to it, or until the planet was removed from the population because it moved too close to the host star and was destroyed. An example of the results of such a run is shown below.
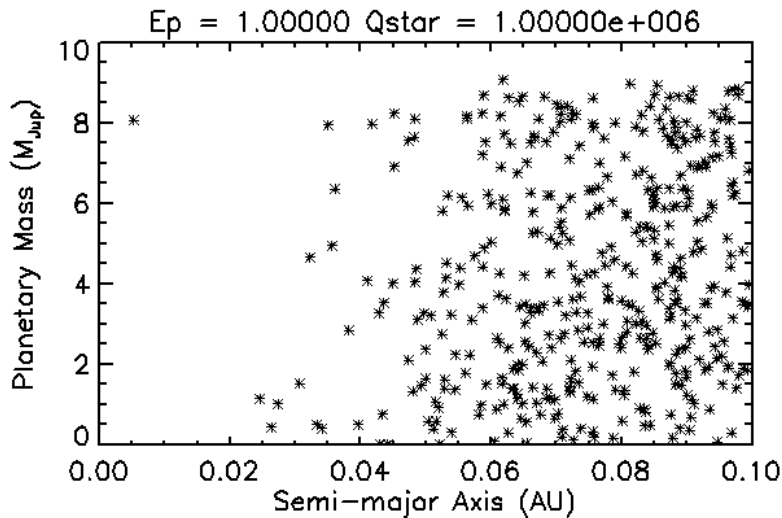

Figure 11: Comparison of Hypothetical Population for ε=1, Q$_*$=10^6. *Graph of the hypothetical population of planets after evolving through the code using an ε value of 1.0 and a Q$_*$ value of 1 x 10^6. There is a thinning out of planets with a < 0.06 AU. Below 0.02 AU there is a cutoff of planets, with a single exception lying around 0.005 AU.*

KS-Test

In order to determine how strongly the hypothetical population resembles the observed population, a 2-dimensional KS-test was used. This is a mathematical test that indicates the probability that two different data sets come from the same distribution. The returned value ranges between 0 and 1, with 0 indicating that there is no chance that the data sets are drawn from the same underlying population, while a score of 1 means the two data sets are statistically indistinguishable.

Before running tests on the data, it is important to set a baseline to see what a good KS-score would be. While a value of 0 and 1 would have a defined meaning, the interpretation of an intermediate value is not as clear. Several examples were generated in order to have a reference frame. To do this, the observed population of exoplanets was compared to both a hypothetical population of planets and a population of planets based on the observed population's parameters.

The first step in this process was going to the online exoplanet encyclopedia and finding all of the planets that were discovered by the radial velocity method and that had a semi-major axis of ≤ 0.1AU. Planets that were missing relevant data were eliminated from the list. In total, 193 planets were left for comparison. A randomly generated population of 193 planets with masses uniformly distributed between 0 and 13 M_{jup} and semi-major axis ≤ 0.1 AU was also created.

To see how similar the two population datasets are, the observed and hypothetical populations were compared using a 2D KS-test. A 2D K-S test code

written by Peter Yoachim at the University of Washington was used to perform this task (http://www.astro.washington.edu/users/yoachim/code.php).

The test comparing a randomly generated population to the observed population was performed 1000 times, which consistently gave extremely low KS-scores. The average value for all of the runs was 8.65×10^{-25}, with a range between 2.38×10^{-35} and 2.43×10^{-22}, indicating, as expected, that the observed M_p and a-values are not uniformly distributed.

The next step was to create random distributions of M_p and a that had the additional criteria that the radial velocity is high enough to fall into detection limits. A program was designed to calculate the radial velocity for each model planetary system and then make an array containing only the masses and semi-major axes that are detectable with modern technology. The High Accuracy Radial Velocity Planet Searcher (HARPS)currently has the best detection capability, with the ability to detect radial velocity shifts on the order of 1 m/s (Dumusque et al., 2011). Applying the requirement that a model planet induced a radial velocity ≥ 1 m/s resulted in the rejection of 1 or 2 value pairs for each population of 193 planets, and so the KS-values were virtually identical to the KS-values of the random population without the addition radial velocity test.

The extremely low values obtained for the KS results led to the question of what a reasonable value would be for a similar population. Two different test cases were run to find values for such a situation. The first test compared two completely random populations. The results of this led to much higher values. After running 1000 tests, the average KS-score was 0.353.

The second case was slightly more involved. Going back to the exoplanet

encyclopedia, the 193 planets used for the original comparison were *again* used. Two populations were made, one where each planetary mass and semi-major axis is set equal to the maximum value allowed by observation of the planet as referenced in the encyclopedia, and the other with the planetary mass and semi-major axis set to the minimum value. For planets that did not have errors given, the values were kept the same as the original. This happened for either the mass or semi-major axis in 44 cases. When the original population was run against the new population derived from the minimum values from the errors, a KS-value of 0.821 was given. Using the maximum value for each parameter gave a KS-value of 0.907. This indicates that a good statistical match would be reflected by a KS-value of 0.8-0.9.

The values given by the KS-test were much lower than these values. The highest, and therefore best-fitting KS-score was 3.01×10^{-31} for an epsilon value of 0.1 and a Q_* value of 10^5. The worst fit was 5.38×10^{-43} for an epsilon value of 0.001 and a Q_* value of 10^6. Comparing the hypothetical population before any evolution occurred with the observed population resulted in a KS-score of 7.06×10^{-39}. The extremely low value of these numbers indicated that a population with an initially random distribution, and then evolved with consideration to flux-driven mass loss and tidal evolution, is not consistent with the observed planets.
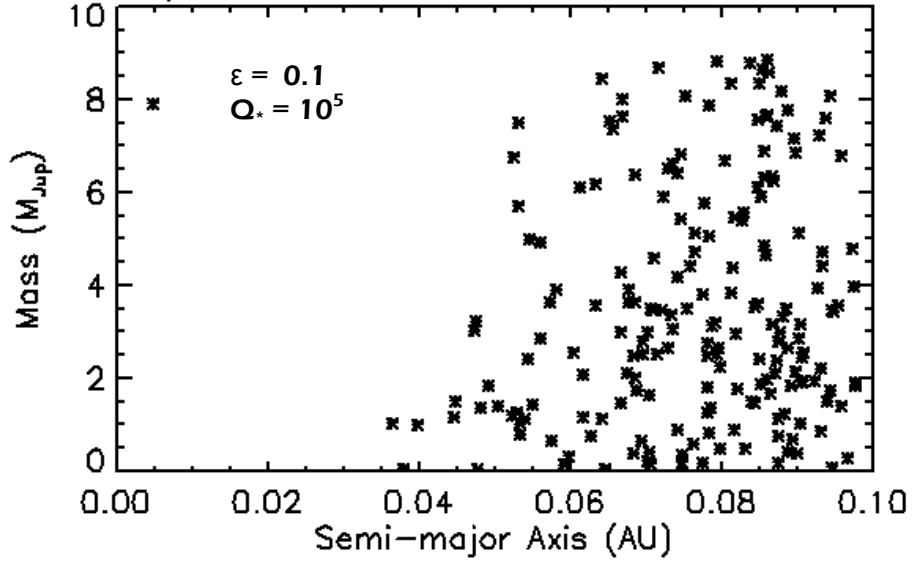
Figure 12: Hypothetical Population with the Highest KS-score. Best fitting hypothetical population after an evolution of ε = 0.1 and Q* = 10d.   The KS-score when compared to the observed population was 3.01 x 10^{-3}
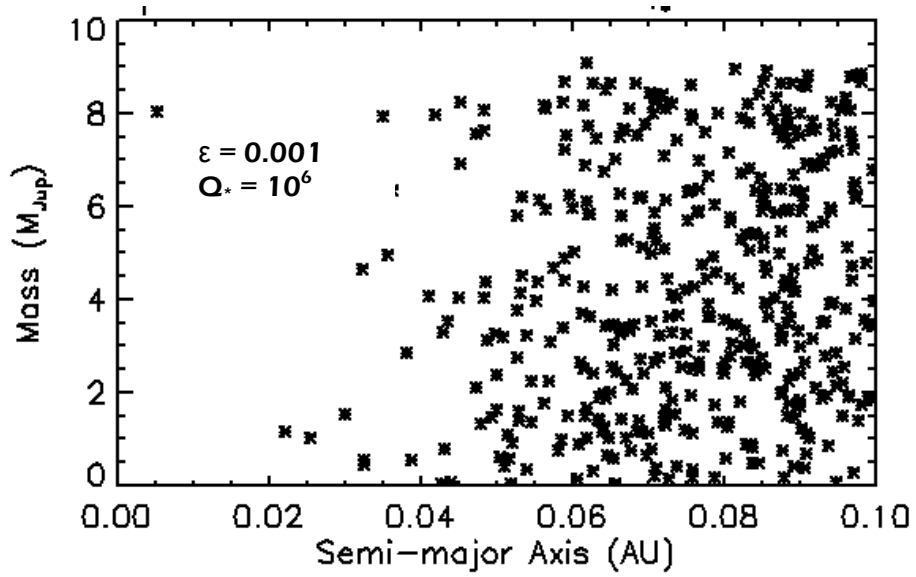

Figure 13: Hypothetical Population with the Lowest KS-score. Worst fitting hypothetical population after evolution with an ε value of near zero and a Q* value of 10^{6}. The KS-score when compared to the observed population was 5.38 x 10^{-43}

CHAPTER IV

CONCLUSION

The effects of atmospheric mass loss and tidal evolution were shown to play an important role in the evolution of close-in exoplanets. The evolution of several sample planets was modeled to see how different initial masses and semi-major axes affect the evolution of planets.

A hypothetical population of planets was then created in order to compare the evolution of a randomly distributed initial population of planets to the observed population. The low KS-scores performed between the hypothetical population (using various assumptions for ε and Q_*) and the observed population indicate that these two populations are statistically inconsistent. This suggests that the original population was not originally formed with an even distribution, or that tides and atmospheric mass loss are not the only effects that shape the planetary distribution.

The absence of hot Jupiter planets closer than twice the distance of their Roche limit suggests that these planets arrived in their present location after moving in to a circular orbit from a more distant elliptical orbit (Ford and Rasio, 2006). This would suggest that the population may be biased toward a larger planetary population than considered here. Conversely, if close-in planets arrive at their destination because of displacement from other planets in the system, the

population may have a population biased toward smaller mass planets.   The implications of these scenarios need to be considered in future work.

The results of this study were surprising, and warrant future research. First, the models used need to be expanded so that planets around non-G type stars can also be included in analysis. Another loose end is determining what initial population would be required in order to reproduce a population similar to what is observed. Several biases in the initial formation of planets, such as a bias in the mass that close-in planets start with, or a tendency of planets of a certain mass to move inwards and become close-in, need to be explored.

REFERENCES

Bouchy, F., Bonomo, A.S., Santerne, A., Moutou, C., Deleuil, M., Diaz, R.F., Eggenbergr, A., Ehrenreich, D., Gry, C., Guillot, T., Havel, M., Hebrard, G., and Udry, S. (2011). SOPHIE Velocimetry of Kepler Transit Candidates. *Astronomy & Astrophysics* 533, A83.

Cecchi-Pestellini, C., Ciaravella, A., Micela, G., and Penz, T. (2009). The Relative Role of EUV Radiation and X-rays in the Heating of Hydrogen-rich Exoplanet Atmospheres. *Astronomy & Astrophysics* 496, pp. 863-868.

Davis, T.A. and Wheatley, P.J. (2009). Evidence for a Lost Population of Close-in Exoplanets. *Monthly Notices of the Royal Astronomical Society* 396, pp. 1012-1017.

DeWarf, L.E., Datin, K.M., and Guinan, E.F. (2010). X-ray, FUV, and UV Observations of α Centauri B: Determination of Long-term Magnetic Activity Cycle and Rotation Period. *The Astrophysical Journal* 722, pp. 343-357.

Dobbs-Dixon, I., Lin, D.N.C., and Mardling, A. (2004). Spin-orbit Evolution of Short-period Planets. *The Astrophysical Journal* 610, pp. 464-476.

Dumusque, X., Santos, N.C., Udry, S., Lovis, C., and Bonfils, X. (2011). Planetary Detection Limits Taking into Account Stellar Noise. *Astronomy & Astrophysics* 527, A82.

Erkaev, N.V., Kulikov, Y.N., Lammer, H., Selsis, F., Langmayr, D., Jaritz, G.F., and Biernat, H.K. (2007). Roche Lobe Effects on the Atmospheric Loss from "Hot Jupiters." *Astronomy & Astrophysics* 472, pp. 329-334.

Fabrycky, D.C., Ford, E.B., Steffen, J.H., Rowe, J.F., Carter, J.A., Moorhead, A.V., Batalha, N.M., Borucki, W.J., Bryson, S., Buchhave, L.A., Christiansen, J.L., Ciardi, D.R., Cochran, W.D., Endl, M., Fanelli, M.N., Fischer, D., Fressin, F., Geary, J., Haas, M.R., Hall, J.R., Holman, M.J., Jenkins, J.M., Koch, D.G., Latham, D.W., Li, J., Lissauer, J.J., Lucas, P., Marcy, G.W., Mazeh, T., McCauliff, S., Quinn, S., Racozzine, D., Sasselov, D., and Shporer, A. (2012). Transit Timing Observations from Kepler: IV. Confirmation of 4 Multiple Planet Systems by Simple Physical Models. In Press, *The Astrophysical Journal*, Accepted Jan 5, 2012.

Ford, E.B., and Rasio, F.A. (2006). On the Relation Between Hot Jupiters and the Roche Limit. *The Astrophysical Journal* 638, pp. L45-L48.

Fortney, J.J., Marley, M.S., and Barnes, J.W. (2007). Planetary Radii Across Five Orders of Magnitude in Mass and Stellar Insolation: Application to Transits. *The Astrophysical Journal* 659, pp. 1661-1672.

Greißmeier, J.M., Stadelmann, A., Penz, T., Lammer, H., Selsis, F., Ribas, I., Guinan, E.F., Motschmann, U., Biernat, H.K., and Weiss, W.W. (2004). The Effect of Tidal Locking on the Magnetospheric and Atmospheric Evolution of "Hot Jupiters." *Astronomy and Astrophysics* 425, pp. 753-762.

Guo, J.H. (2010). The Effect of Mass Loss on the Tidal Evolution of Extrasolar Planets. *The Astrophysical Journal* 712, pp. 1107-1115.

Habets, G.M.H.J., and Heintze, J.R.W. (1981). Empirical Bolometric Corrections for the Main-Sequence. *Astronomy & Astrophysics Supplement Series* 46, pp. 193-237.

Harris, D.L., Strand, K.A., and Worley, C.E. (1963). Empirical Data on Stellar Masses, Luminocities and Radii. *Basic Astronomical Data – Stars and Stellar Systems III.* (ed. K. Strand). Chicago: University of Chicago Press.

Hellier, C., Anderson, D.R., Collier-Cameron, A., Miller, G.R.M., Queloz, D... and Triaud, A.H.M.J. (2011). On the Orbit of the Short-period Exoplanet WASP-19b. *The Astrophysical Journal Letters* 730, L31.

Hubbard, W.B., Hattori, M.F., Burrows, A., Hubeny, I., and Sudarsky, D. (2007a). Effects of Mass Loss for Highly-Irradiated Giant Planets. *Icarus* 187, pp. 358-364.

Hubbard, W.B., Hattori, M.F., Burrows, A., and Hubeny, I. (2007b). A Mass function Constraint on Extrasolar Giant Planet Evaporation Rates. *The Astrophysical Journal* 658, pp. L59-L62.

Ivanova, N. and Taam, R.E. (2003). Magnetic Braking Revisited. *The Astrophysical Journal* 599, pp. 516-521.

Jackson, B., Miller, N., Barnes, R., Raymond, S.N., Fortney, J.J., and Greenberg, R. (2010). The Roles of Tidal Evolution and Evaporative Mass Loss in the Origin of CoRoT-7 b. *Monthly Notices of the Royal Astronomical Society* 407, pp. 910-922.

Kulikov, Y.N., Lammer, H., Lichtenegger, H.I.M., Terada, N., Ribas, I., Kolb, C., Langmayr, D., Lundin, R., Guinan, E.F., Barabash, S., and Biernat, H.K. (2006). Atmospheric and Water Loss from Early Venus. *Planetary and Space Science* 54, pp. 1425-1444.

Lammer, H., Selsis, F., Ribas, I., Guinana, E.F., Bauer, S.J., and Weiss, W.W. (2003). Atmospheric Loss of Exoplanets Resulting From Stellar X-ray and Extreme-Ultraviolet Heating. *The Astrophysical Journal* 598, pp. L121-L124.

Lammer, H., Odert, P., Leitzinger, M., Khodachenko, M.L., Panchenko, M., Kulikov, Y.N., Zhang, T.L., Lichtenegger, H.I.M., Erkaev, N.V., Wucherl, G., Micela, Penz, T., Biernat, H.K., Weingrill, J., Steller, M., Ottacher, H., Hasiba, J., and Hanslmeier, A. (2009). Determining the Mass Loss Limit for Close-in Exoplanets: What Can We Learn from Transit Observations? *Astronomy & Astrophysics* 506, pp. 399-410.

Lang, K.R. (1992). *Astrophysical Data: Planets and Stars*. Springer-Verlag New York, Inc.

Lecavelier des Etangs, A. (2007). A Diagram to Determine the Evaporation Status of Extrasolar Planets. Astronomy & Astrophysics 461, pp. 1185-1193.

Lin, D., Bodenheimer, P., and Richardson, D. (1996). Orbital Migration of the Planetary Companion of 51 Pegasi to its Present Location. *Nature*, Vol. 380, Issue 6575, pp. 606-607.

Miller, N., Fortney, J.J., and Jackson, B. (2009). Inflating and Deflating Hot Jupiters: Coupled Tidal and Thermal Evolution of Known Transiting Planets. *The Astrophysical Journal* 702, pp. 1413-1427.

Murray, C.D., and Dermott, S.F. (1999). *Solar System Dynamics*. Cambridge University Press.

Murray-Clay, R.A., Chiang, E.I., and Murray, N. (2009). Atmospheric Escape from Hot Jupiters. *The Astrophysical Journal* 693, pp. 23-42.

Ogilvie, G.I., and Lin, D.N.C. (2007). Tidal Dissipation in Rotating Solar-Type Stars. *The Astrophysical Journal* 661, pp.1180-1191.

Penev, K., and Sasselov, D. (2011). Tidal Evolution of Close-in Extrasolar Planets: High Stellar Q From New Theoretical Models. *The Astrophysical Journal* 731, pp. 67-71.

Penz, T., Micela, G., and Lammer, H. (2008). Influence of the Evolving Stellar X-ray Luminocity Distribution on Exoplanetary Mass Loss. *Astronomy & Astrophysics* 477, pp. 309-314.

Pizzolato, N., Maggio, A., Micela, G., Sciortino, S., and Ventura, P. (2003). The Stellar Activity-rotation Relationship Revisited: Dependence of Saturated and Non-saturated X-ray Emission Regime son Stellar Mass for Late-type Dwarfs. *Astronomy & Astrophysics* 397, pp. 147-157.

Quinn, S.N., Bakos, G.A., Hartman, J., Torres, G., Kovacs, G... and Sari, P. (2012). HAT-P-25b: A Hot-Jupiter Transiting a Moderately Faint G Star. *The Astrophysical Journal* 745, pp. 80.

Rasio, F.A., Tout, C.A., Lubow, S.H., and Liviio, M. (1996). Tidal Decay of Close Planetary Orbits. *The Astrophysical Journal* 470, pp. 1187-1191.

Ribas, I., Guinana, E.F., Güdel, M., and Audard, M. (2005). Evolution of the Solar Activity Over Time and Effects on Planetary Atmospheres. I. High-Energy Irradiances (1-1700 Å). *The Astrophysical Journal* 622, pp. 680-694.

Rogers, L.A., and Seager, S. (2010). Three Possible Origins for the Gas Layer on GJ 1214b. *The Astrophysical Journal* 716, pp. 1208-1216.

Sanz-Forcada, J., Ribas, I., Micela, G., Pollock, A.M.T., Garcia-Alvarez, D., Solano, E., and Eiroa, C. (2010). A Scenario of Planet Erosion by Coronal Radiation. *Astronomy & Astrophysics* 511, L8.

Sanz-Forcada, J., Micela, G., Ribas, I., Pollock, A.M.T., Eiroa, C., Velasco, A., Solano, E., and García-Álvarez, D. (2011). Estimation of the XUV Radiation Onto Close Planets and Their Evaporation. *Astronomy & Astrophysics* 532, A6.

Simon, T., Herbig, G., and Boesgaard, A.M. (1985). The Evolution of Chromospheric Activity and the Spin-down of Solar-type Stars. *The Astrophysical Journal* 293, pp. 551-574.

Skumanich, A. (1972). Time Scales for Ca II Emission Decay, Rotational Braking, and Lithium Depletion. *The Astrophysical Journal* 171, pp. 565-567.

Takeda, G., Ford, E.B., Sills, A., Rasio, F.A., Fischer, D.A., and Valenti, J.A. (2007). Structure and Evolution of Nearby Stars with Planets. II. Physical Properties of ~ 1000 Cool Stars from the SPOCS Catalog. *The Astrophysical Journal Supplement Series* 168, pp. 297-318.

Yelle, R.V. (2004). Aeronomy of Extra-Solar Giant Planets at Small Orbital Distances. *Icarus* 170, pp. 167-179.

Zahnle, K.J., and Walker, J.C.G. (1982). The Evolution of Solar Ultraviolet Luminocity. *Reviews of Geophysics* 20, No. 2, pp. 280-292.